Molecular dynamics study of oxygen diffusion in Pr_2NiO_{4+}

Molecular dynamics study of oxygen diffusion in $Pr_2NiO_{4+\delta}$

David Parfitt, Alexander Chroneos,* John A. Kilner and Robin W. Grimes

Received 27th January 2010, Accepted 17th March 2010
First published as an Advance Article on the web 11th May 2010
DOI: 10.1039/c001809k

Oxygen transport in tetragonal $Pr_2NiO_{4+\delta}$ has been investigated using molecular dynamics simulations in conjunction with a set of Born model potentials. Oxygen diffusion in $Pr_2NiO_{4+\delta}$ is highly anisotropic, occurring almost entirely *via* an interstitialcy mechanism in the *a–b* plane. The calculated oxygen diffusivity has a weak dependence upon the concentration of oxygen interstitials, in agreement with experimental observations. In the temperature range 800–1500 K, the activation energy for migration varied between 0.49 and 0.64 eV depending upon the degree of hyperstoichiometry. The present results are compared to previous work on oxygen self-diffusion in related K_2NiF_4 structure materials.

Introduction

Perovskite and related materials of the Ruddlesden–Popper (RP) series of layered oxides (formula $A_{n+1}B_nO_{3n+1}$) are promising candidate materials for intermediate temperature solid-oxide fuel cell cathodes, separation membranes, and oxygen sensors.[1–4] The first members of the RP series, A_2BO_4, such as Pr_2NiO_4 exhibit desirable electrochemical, catalytic and electrical properties combined with mechanical and thermal stability.

In general praseodymium containing perovskite oxides are of interest due to their high performance: $Pr_2NiO_{4+\delta}$ has considerable potential merit due to its very high oxygen diffusion, as observed by Boehm *et al.*[5] in conjunction with its desirable cathodic properties. We also note that the value of oxygen diffusion in related compounds such as $PrBaCo_2O_{5+\delta}$ is considerably higher than in $GdBaCo_2O_{5+\delta}$ and other simple perovskite materials.[6] It is of interest therefore to explore the origin of the increased performance of these materials: Is the enhanced diffusivity a basic property of praseodymium-containing compounds?

Our previous work[3] on the isostructural compound $La_2NiO_{4+\delta}$ has demonstrated the efficacy of molecular dynamics (MD) simulations in identifying the mechanism of oxygen ion diffusion. In this work we examine the case of $Pr_2NiO_{4+\delta}$ with the intent to examine the magnitude of the diffusivity, elucidate the diffusion mechanism and compare it to the case of $La_2NiO_{4+\delta}$. We investigate the dependence of the oxygen ion diffusivity upon the degree of hyperstoichiometry and comment upon the origin of the unusually weak dependence of the diffusivity on the oxygen interstitial concentration. Finally, we examine the results of the simulations in the context of the wider behaviour of A_2BO_4 type oxides.

Methods

To examine the behaviour of the conduction mechanism in $Pr_2NiO_{4+\delta}$ we have employed a series of MD simulations using effective pair potentials to replicate the interaction between ions. The evolution of the simulation proceeds *via* iterative numerical solution of Newton's equations from pre-determined starting configurations. Within the constraints of classical mechanics and the pair potential model employed this behaviour should mimic the short timescale evolution of the real material.

The success of the molecular dynamics technique depends upon an accurate description of the energy of a unique atomic configuration. In this case the ionic lattice of $Pr_2NiO_{4+\delta}$ is described using Born's model.[7] Ions *i* and *j* of formal charge q_i and q_j interact by a long-range Coulombic potential (summed using Ewald's method)[8] and a short-range parameterized Buckingham pair potential.[9] The latter is summed to the cut-off value of 10.5 Å, beyond which the influence of the potential is considered negligible. The combined lattice energy is given by,

$$E_L = \sum_{j>i} \sum \left[\frac{q_i q_j}{4\pi\varepsilon_0 r_{ij}} + A_{ij} \exp\left(\frac{-r_{ij}}{\rho_{ij}}\right) - \left(\frac{C_{ij}}{r_{ij}^6}\right) \right] \quad (1)$$

where r_{ij} is the interionic separation, A_{ij}, ρ_{ij} and C_{ij} are the short-range parameters of the Buckingham pair potential and ε_0 is the permittivity of free space. Table 1 details the parameters used in the simulations. The efficacy of the parameters used has been established for Pr_2NiO_4 as the calculated unit cell volume is within 0.74% of the determined value (maximum percent difference of the lattice parameters is 1.75%),[5] whereas the oxygen–oxygen interaction has been successfully used in a number of oxides.[10–12]

Initial configurations for a given stoichiometry were created from a $10 \times 10 \times 4$ supercell of the experimentally determined structure of $Pr_2NiO_{4+\delta}$. Additional oxygen ions were assigned at a random sample of interstitial sites within the crystal, the

Table 1 Buckingham interionic potential parameters (see eqn (1))

Interaction	A_{ij}/eV	ρ_{ij}/Å	C_{ij}/eV Å^6
O^{2-}–O^{2-}	9547.96	0.2072	32.00
Pr^{3+}–O^{2-}	2025.54	0.3427	13.85
Ni^{2+}–O^{2-}	905.40	0.3145	0.00

Department of Materials, Imperial College London, London, UK SW7 2AZ

total number of ions in the simulations were therefore 5600 + 800δ for a particular stoichiometry. We used a uniformly charged background to compensate for the interstitial–interstitial interactions. Ion velocities were initially assigned along random directions and with a magnitude distribution consistent with a Maxwell–Boltzmann distribution at the specified temperature.

Simulations were performed using DLPOLY version 3.09, we used a velocity verlet algorithm for the integration of the forces.[13] A Nosé–Hoover thermostat and barostat[14,15] were used to correct the thermal average temperature and strain in the appropriate ensemble. Each simulation was equilibrated for 5000 timesteps (5 ps) at each temperature and stoichiometry before a longer 25 000 timestep (25 ps) simulation under a constant pressure ensemble was performed to establish the average cell parameters. A production run of up to 250 000 timesteps (250 ps) in a constant volume ensemble at the thermodynamic average cell parameters was used to collect statistical information about the diffusion rates. The visual molecular dynamics package VMD[16] was used in the production of the figures.

Results and discussion

In the temperature range of interest for solid oxide fuel cells $Pr_2NiO_{4+\delta}$ (and $La_2NiO_{4+\delta}$) exist as a tetragonal structure.[17,18] At temperatures below 720 K $Pr_2NiO_{4+\delta}$ transforms into an orthorhombic symmetry.[19] The structure of Pr_2NiO_4 in its tetragonal form is illustrated in Fig. 1, it can be considered as a combination of perovskite ($PrNiO_3$ units) layers intergrown with PrO rocksalt-type layers. A perfect match of these layers would result in the tetragonal *I*4/*mmm* space group.[18] However, there is considerable mismatch between these layers and therefore significant stress in the unrelaxed case. The interlayer mismatch promotes the formation of oxygen interstitials in the Pr_2O_2 bilayers.[19] The mismatch between layers is more significant for $Pr_2NiO_{4+\delta}$ than $La_2NiO_{4+\delta}$ as praseodymium is smaller compared to lanthanum.[19] Within the *I*4/*mmm* space group we identify three distinct oxygen sites. The equatorial and apical sites, which make up the NiO_6 octahedra, are located at (0, 1/2, 0) (4(c)) and (0, 0, 0.1773) (4(e)), respectively. The interstitial sites, at (1/4, 1/4, 0.22), are four-fold coordinated to the Pr sites.

The incorporation of the oxygen interstitials into the Pr_2O_2 bilayers causes a local distortion of the NiO_6 octahedra, shown schematically in Fig. 1. The driving force for this is the Coulombic repulsion between apical ions terminating the NiO_6 perovskite layers and the interstitial ion itself. The distortion removes the original local symmetry of the unit cell, though as we will show the diffusion process produces a unit cell that is, on average, consistent with the original designated unit cell.

The average oxygen ion density was calculated by averaging the positions of the oxygen ions over the 250 ps of the simulations and mapping the 10 × 10 × 4 supercell positions back to a set of fractional unit cell coordinates. The results for δ = 0.09875 and a temperature of 1100 K are shown in Fig. 1. We first note the similarity of this oxygen ion distribution to

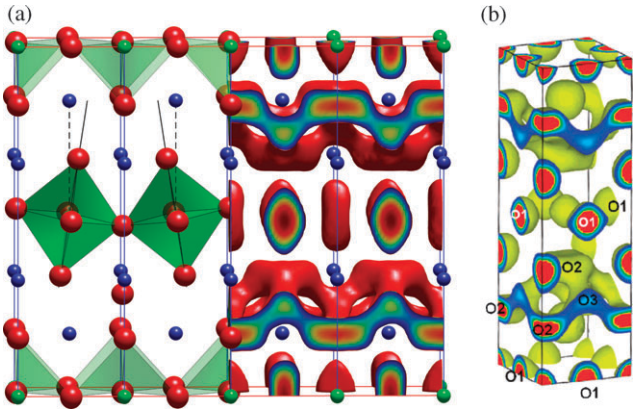

Fig. 1 (a) The crystal structure of $Pr_2NiO_{4+\delta}$ (O ions in red, NiO_6 octahedra in green and Ni ions in blue, the *c*-axis is the vertical axis) and the isosurface connecting the O diffusion sites in the *a*–*b* plane from MD at 1100 K and δ = 0.09875 (b) comparison with maximum entropy method results (reprinted with permission form ref. 2. Copyright 2008, American Chemical Society).

previous calculated results for $La_2NiO_{4+\delta}$; this is to be expected due to the similarity in structure and chemistry between the two compounds.[3] The dominant mechanism of oxygen ion transport is *via* the network of apical oxygen sites connected by interstitial ion sites. These form the continuous, energetically accessible network of partially occupied sites necessary for bulk ionic diffusion.

Interestingly, Yashima *et al.*[2] recently provided experimental evidence for an interstitial mechanism in the related tetragonal $(Pr_{0.9}La_{0.1})_2(Ni_{0.74}Cu_{0.21}Ga_{0.05})O_{4+\delta}$. In their study, Yashima *et al.*[2] used neutron scattering experiments and analysis based on the maximum entropy method to demonstrate that oxygen atoms move *via* an interstitial process along a two-dimensional network in the *a*–*b* plane. Diffusion of O^{2-} ions across the *a*–*b* plane is also consistent with the MD studies of Savvin *et al.*[20] in tetragonal $La_{2-x}Sr_xCuO_{4-\delta}$ and our recent work on tetragonal $La_2NiO_{4+\delta}$.[3] Fig. 1 shows the predicted oxygen ion density which is a remarkably similar profile to that predicted from maximum entropy analysis of diffraction data. We note the highly anisotropic ellipsoids of the equatorial oxygen ions, flattened and elongated along the *c*-axis and the 'peanut' shaped split apical oxygen sites similar to those observed by Allançon *et al.*[18] Although appearing highly disordered, the occupancies of the apical sites are strongly correlated. The oxygen ions and their associated NiO_6 octahedra tend to tilt away from any adjacent interstitial oxygen site such as to minimise the oxygen–oxygen Coulomb repulsion. This tilting of the four NiO_6 octahedra away from the interstitial oxygen ion means that the oxygen ions on the apical sites on the opposite end of the octahedron move slightly closer together. These apical sites lie in the rocksalt layers above and below that containing the interstitial and the tilting movement is now towards vacant interstitial sites in these adjacent layers. A likely consequence is that this will make these sites in the adjacent layers less likely to be occupied by further oxygen ions. Depending upon how far this relaxation propagates through the structure, the interstitials will begin to interact, leading to correlated motion at high temperatures and perhaps

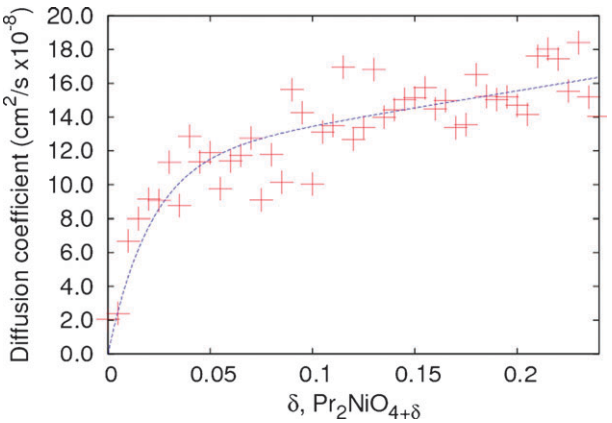

Fig. 2 Diffusion coefficient with respect to the oxygen hyperstoichiometry.

the onset of ordered structures as have been observed at low temperatures by electron microscopy.[21]

The oxygen ion diffusivity in $Pr_2NiO_{4+\delta}$ is highly anisotropic with almost all of the migration taking place in the *a–b* planes (Fig. 1). The diffusion process is similar to the interstitialcy mechanism predicted for $La_2NiO_{4+\delta}$.[3,22] It proceeds *via* the promotion of an apical oxygen ion into an adjacent interstitial site leaving a vacant site on one of the NiO_6 octahedra. This vacant site is then filled by a second neighbouring interstitial site. As a very rare event the vacant apical site was filled by a equatorial oxygen ion which was able to move between adjacent layers, however this occurred only a few times during the entire 250 ps of the simulations. Consequently, it was not possible to obtain meaningful statistics on the levels of *c*-axis conduction other than it is many orders of magnitude less than transport in the *a–b* plane.

Oxygen diffusivities were calculated for a range of hyperstoichiometries. There is excellent agreement between the absolute calculated values and those observed experimentally. Calculated values for the activation energy of migration from these simulations depend upon the degree of hyperstoichiometry and range from 0.49 eV ($\delta = 0.025$) to higher values 0.64 eV ($\delta = 0.20$). In the case of experiment the sample stoichiometry is itself a function of temperature and the surrounding atmosphere. Nevertheless the experimental values for the activation energy of migration, 0.6 eV,[5] is within the range of values predicted from these calculations.

To examine in greater detail the dependence of the diffusivity upon the stoichiometry of $Pr_2NiO_{4+\delta}$ we show in Fig. 2 the diffusivity plotted as a function of delta for a series of simulations at 1100 K. The oxygen diffusivity, D, at a temperature T is given by, $D = [O_i]f\exp(-E_m/k_BT)$. Here $[O_i]$ is the concentration of oxygen interstitials, f is the correlation factor which we assume to be constant, E_m is the energy barrier to migration and k_B is Boltzmann's constant. From Fig. 2 we see that initially the diffusivity rises rapidly as we increase the concentration of oxygen interstitials. However, beyond approximately $\delta \sim 0.02$ the diffusivity levels off. We interpret this as a rise in the effective migration barrier due to two effects: (i) the increased formation energy of oxygen interstitials due to the presence of other pre-existing neighbouring interstitials and (ii) a stiffening of the lattice cause by the additional oxygen interstitial effectively pinning the NiO_6 sub-lattice, which in turn reduces the ease with which the octahedra can tilt to accommodate passage of the oxygen ions. The predicted variation in the diffusivity for specific δ value is due to the different population of oxygen interstitials along the layers.

Conclusions

In conclusion we predict that oxygen diffusion in $Pr_2NiO_{4+\delta}$ is highly anisotropic, occurring almost entirely *via* an interstitialcy mechanism in the *a–b* plane, although a limited vacancy transport mechanism was also identified along the *c*-axis. The calculated oxygen diffusivity has a weak dependence upon the concentration of oxygen interstitials, in agreement with experimental observations. In the temperature range 800–1500 K, the activation energy for migration varied between 0.49 and 0.64 eV depending upon the degree of hyperstoichiometry. The origin of the observed weak variation of diffusivity upon the degree of hyperstoichiometry is explained in terms of the stiffening of the NiO_6 octahedral sublattice.

The study was supported by EP/F009720/1 "New Research Directions for Solid Oxide Fuel Cell Science and Engineering". Computing resources were provided by the HPC facility of Imperial College London.

References

1 V. V. Vashook, N. E. Trofimenko, H. Ullmann and L. V. Makhnach, *Solid State Ionics*, 2000, **131**, 329.
2 M. Yashima, M. Enoki, T. Wakita, R. Ali, Y. Matsushita, F. Izumi and T. Ishihara, *J. Am. Chem. Soc.*, 2008, **130**, 2762.
3 A. Chroneos, D. Parfitt, J. A. Kilner and R. W. Grimes, *J. Mater. Chem.*, 2010, **20**, 266.
4 D. Rupasov, A. Chroneos, D. Parfitt, J. A. Kilner, R. W. Grimes, S. Ya. Istomin and E. V. Antipov, *Phys. Rev. B: Condens. Matter Mater. Phys.*, 2009, **79**, 172102.
5 E. Boehm, J. M. Bassat, P. Dordor, F. Mauvy, J. C. Grenier and Ph. Stevens, *Solid State Ionics*, 2005, **176**, 2717.
6 G. Kim, S. Wang, A. J. Jacobson, L. Reimus, P. Brodersen and C. A. Mims, *J. Mater. Chem.*, 2007, **17**, 2500.
7 M. Born and J. E. Mayer, *Z. Phys.*, 1932, **75**, 1.
8 P. P. Ewald, *Ann. Phys.*, 1921, **369**, 253.
9 R. A. Buckingham, *Proc. R. Soc. London, Ser. A*, 1938, **168**, 264.
10 R. W. Grimes, G. Busker, M. A. McCoy, A. Chroneos, J. A. Kilner and S. P. Chen, *Ber. Bunsen-Ges. Phys. Chem.*, 1997, **101**, 1204.
11 G. Busker, A. Chroneos, R. W. Grimes and I. W. Chen, *J. Am. Ceram. Soc.*, 1999, **82**, 1553.
12 M. R. Levy, C. R. Stanek, A. Chroneos and R. W. Grimes, *Solid State Sci.*, 2007, **9**, 588.
13 W. C. Swope, H. C. Andersen, P. H. Berens and K. R. Wilson, *J. Chem. Phys.*, 1982, **76**, 637.
14 S. Nosé, *J. Chem. Phys.*, 1984, **81**, 511.
15 W. G. Hoover, *Phys. Rev. A: At., Mol., Opt. Phys.*, 1985, **31**, 1695.
16 W. Humphrey, A. Dalke and K. Schulten, *J. Mol. Graphics*, 1996, **14**, 33.
17 S. J. Skinner, *Solid State Sci.*, 2003, **5**, 419.
18 C. Allançon, J. Rodríguez-Carvajal, M. T. Fernández-Díaz, P. Odier, J. M. Bassat, J. P. Loup and J. L. Martínez, *Z. Phys. B: Condens. Matter*, 1996, **100**, 85.
19 A. J. D. Sullivan, D. J. Buttrey, D. E. Cox and J. Hriljac, *J. Solid State Chem.*, 1991, **94**, 337.
20 S. N. Savin, G. N. Mazo and A. K. Ivanov-Schitz, *Crystallogr. Rep.*, 2008, **53**, 291.
21 M. J. Sayagués, M. Vallet-Regí, J. L. Hutchison and J. M. González-Calbet, *J. Solid State Chem.*, 1996, **125**, 133.
22 A. Chroneos, R. V. Vovk, I. L. Goulatis and L. I. Goulatis, *J. Alloys Compd.*, 2010, **494**, 190.

